MODELING THE RESPONSE OF THE MEDITERRANEAN SEA LEVEL TO GLOBAL AND REGIONAL CLIMATIC PHENOMENA

D.A. Natsiopoulos [(1)], G.S. Vergos [(2)], I.N Tziavos [(3)]

[(1)] *Aristotle University of Thessaloniki, Department of Geodesy and Surveying, Thessaloniki, GR-54124, Greece, Email: dnatsio@topo.auth.gr*
[(2)] *Aristotle University of Thessaloniki, Department of Geodesy and Surveying, Thessaloniki, GR-54124, Greece, Email: vergos@topo.auth.gr*
[(3)] *Aristotle University of Thessaloniki, Department of Geodesy and Surveying, Thessaloniki, GR-54124, Greece, Email: tziavos@topo.auth.gr*

ABSTRACT

The exploitation of satellite altimetry data from past and current satellite missions is crucial to both oceanographic and geodetic applications. This work presents a correlation analysis of Jason-1, Jason-2 and CryoSat-2 Sea Level Anomalies (SLAs) with global and regional climatic indexes that influence the ocean state. The Southern Oscillation Index, North Atlantic Oscillation index and Mediterranean Oscillation Index have been investigated, as representative of climate-change and seasonal forcing on the sea level. The raw data used are SLA values from Jason-1, Jason-2 (2002-2014) and CryoSat-2 (2010-2014) over the entire Mediterranean Basin. The possible correlation is investigated in seasonal and monthly scale, while a regional multiple regression and a principal component analysis between the SLAs and oscillation indexes is carried out. Finally, evidence of the sea level cyclo-stationarity in the Mediterranean Sea is deduced from the analysis of empirically derived covariance functions at monthly intervals from the available SLA data.

1. INTRODUCTION

Satellite altimetry data sets offer an abundance of, unprecedented in accuracy and resolution, data from past and current missions being is crucial to both oceanographic and geodetic applications. For oceanographic studies they allow the determination of Sea Level Anomalies (SLA), as deviations from a static mean sea level, while they are also fundamental for marine geoid and gravity determination. This work presents correlations of the SLA with global and regional climatic phenomena that influence the ocean state. Three such indexes have been investigated. The first one is the well-known Southern Oscillation Index (SOI) corresponding to the ocean response to El Niño/La Niña-Southern Oscillation (ENSO) events [4]. The next index investigated is the North Atlantic Oscillation (NAO) index, which corresponds to the fluctuations in the difference of atmospheric pressure at sea level between the Icelandic low and the Azores high [18]. The last index investigated is the Mediterranean Oscillation Index (MOI), which refers to the fluctuations in the difference of atmospheric pressure at sea level between Algiers and Cairo [6]. In order to investigate possible correlations between climate-induced changes and altimetry-derived SLAs, the covariance functions of the latter are used as representative of the statistical characteristics of the sea state.

2. DATA USED AND CORRECTIONS

The raw data used are SLA values from Jason-1 and Jason-2 (Fig. 1-right) for a period of thirteen years (2002-2014) and from CryoSat-2 (Fig.1-left) for a period of 5 consecutive years 2010-2014 within the entire Mediterranean Basin ($30° \leq \varphi \leq 50°$ and $-10° \leq \lambda \leq 40°$). For Jason-1, data during the period from 15/1/2002 (cycle 1) to 07/12/2008 (cycle 255) have been used resulting in a total number of 670703 observations. For Jason-2, data from 4/7/2008 (cycle 0) to 31/12/2014 (cycle 239) have been used with a total number of 882197 observations. Finally, Cryosat-2 data during the period from 14/07/2010 (cycle 4) to 31/12/2014 (cycle 61) resulting in a total number of 653131 SLA values. Each Jason-1 and Jason-2 cycle consists of 254 passes with almost 15% of those having available observations in the Mediterranean Sea within the satellite's period of 10 days. For each year 36 cycles and ~92000 observations are available with a cross track spacing of 300km at the equator while CryoSat-2 has a 369 day orbit with a cross track spacing of 7.5 km at the equator and ~142000 observations per year within the Mediterranean.

The data have been downloaded from RADS server (DEOS Radar Altimetry Data System) in the form of SLAs relative to a zero-tide EGM2008 geoid, after applying all the necessary geophysical and instrumental corrections [2], [3], [17], [19]. The so-derived altiemtric SLAs has been used to investigate possible correlations with global and regional climatic phenomena. For the present study, NAO, SOI and MOI data have been acquired from the Climate Research Unit of the University of East Anglia [5].

Proc. 'Living Planet Symposium 2016', Prague, Czech Republic, 9–13 May 2016 (ESA SP-740, August 2016)

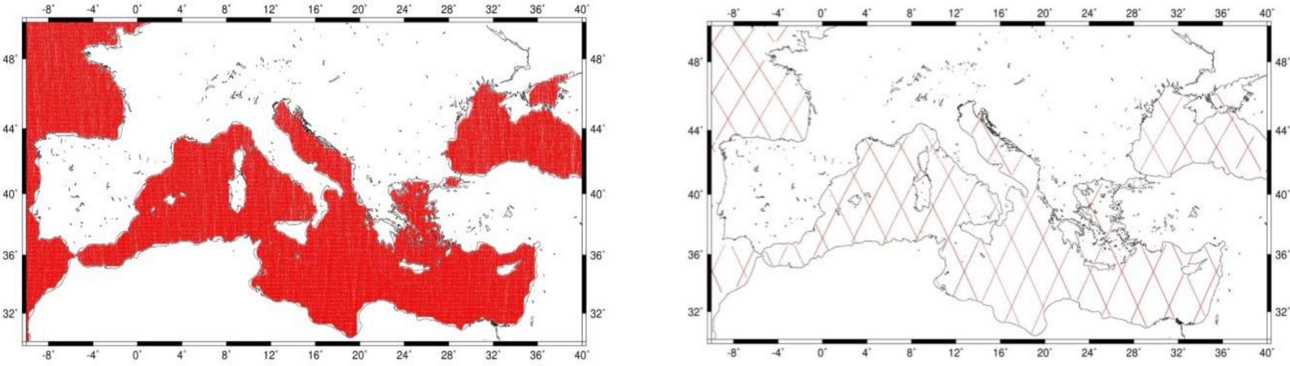

Figure 1: Cryosat-2 (left) and Jason (right) data distribution over the Mediterranean Sea

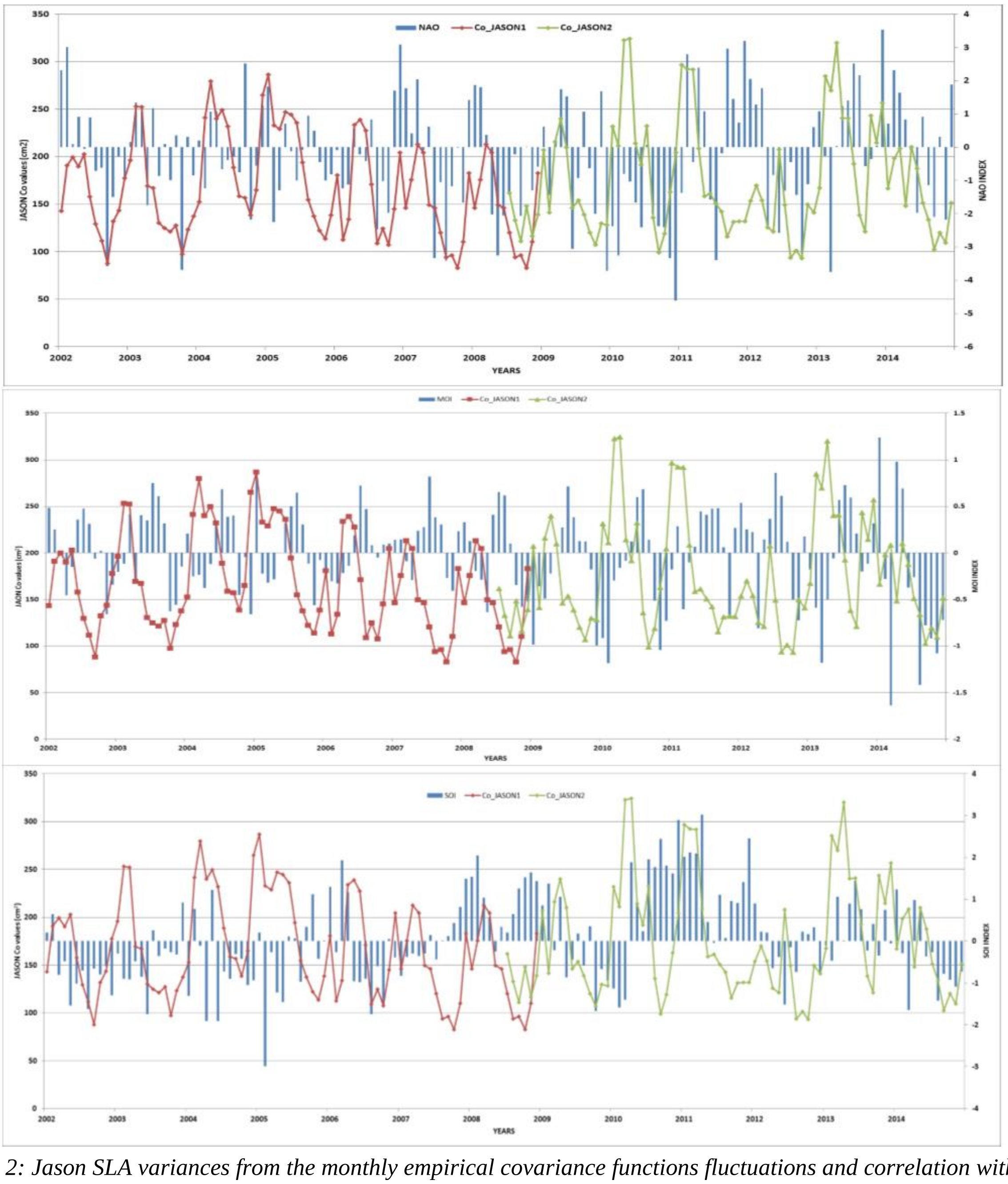

Figure 2: Jason SLA variances from the monthly empirical covariance functions fluctuations and correlation with NAO (top), MOI (middle) and SOI (bottom).

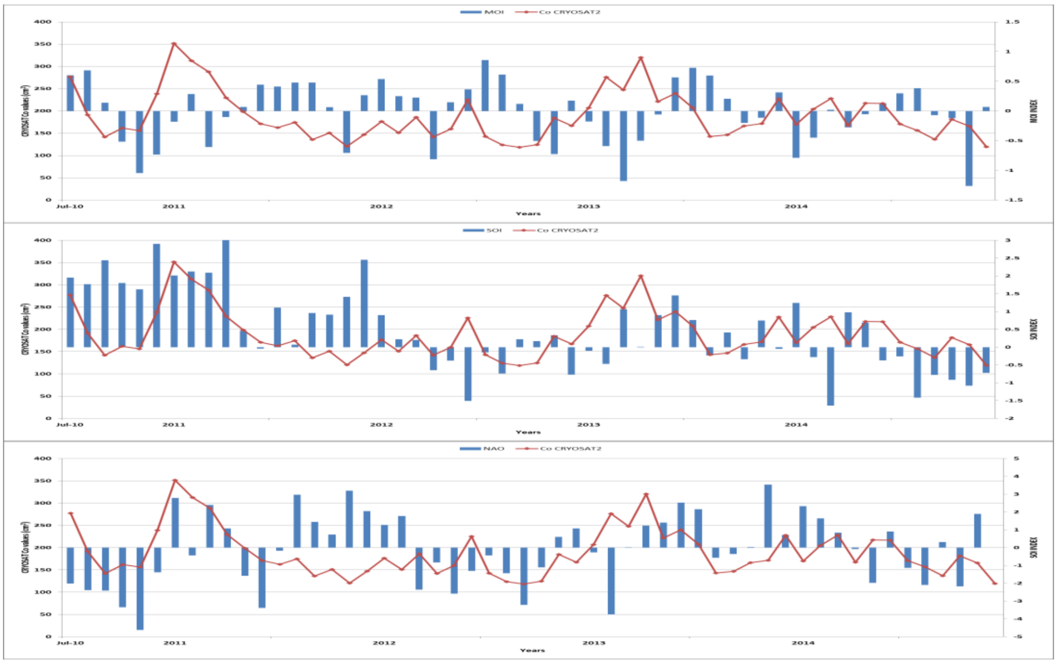

Figure 3: Cryosat-2 SLA variances from the monthly empirical covariance functions fluctuations and correlation with MOI (top), SOI (middle) and NAO (bottom).

3. COVARIANCES AS A TOOL FOR THE ANALYSIS OF SLA

As pointed out in the introduction, the available SLAs will be used to calculate the variance as an indicator for the time variations of the SLA itself and this can be further correlated with large-scale regional and global climatic phenomena. The Tscherning and Rapp model was fitted to the variance of SLA derived from the available data for each satellite in monthly scale [24]. If each observation y_i represent a small area A_i and y_j represents an area A_j then the empirical covariance is:

$$C(\psi) = \frac{\sum A_i A_j y_i y_j}{\sum A_i A_j}, \quad (1)$$

with $\psi_{k-1} < \psi_{ij} < \psi_k$ where ψ is the spherical distance.
If the area is subdivided into small cells holding one observation each and A_i and A_j are assumed to be equal then Eq. 1 reduces to

$$C_k = \frac{\sum y_i y_j}{N_k}, \quad (2)$$

where N_k is the number of products $y_i\, y_j$ in the k^{th} interval [11]. From Eq. 2, the variance C_o is equal to

$$C_0 = \frac{\sum y_i y_j}{N}, \quad (3)$$

In Fig. 2 below the Jason SLA variances from the monthly empirical covariance functions are presented along with the fluctuations of NAO (top), MOI (middle) and SOI (bottom). As it can be seen, MOI is the most proper measure of atmospheric forcing contribution to sea level variations in the Mediterranean. From Fig.2 and Fig.3 it is clear that positive phases in MOI are related to depressions in the SLA due to dryer conditions, as for example during the summer period of 2002-2004, 2006-2008 and 2009-2014. The same behaviour can be seen for the negative MOI values, which result in increased sea levels as for example in early 2002, 2004-2007, 2010-2011, 2013 and late 2014 for Cryosat-2 [16], [22], [23], [26], [29].

From Fig. 2 and Fig.3 it is also noticed that there is correlation between ENSO events and SLA variations in the Mediterranean with a phase offset of 3-6 months. The large negative values of the SOI index at the beginning of 2004 and 2005 are related to the large variance values which appear in spring of 2004 and in summer of 2005, respectively. The weak El Niño in March 2006 has a more rapid signature in the Mediterranean Sea with a significant increase in the SLA in June-July 2006, i.e., a time period of 5 months. The same behaviour is evidenced for the La Niña events too, as it can be seen for the moderate occurrences in late 2007-early 2008 and in late 2010 and early 2011. These result in significant depressions in the SLA variances, which reach their smallest values in summer 2008 and in spring 2011, i.e., with a time lag of ~3-5 months [1], [12], [21]. Due to the distance between the Equatorial Pacific, where ENSO events take place, and the Mediterranean SOI may not be the appropriate index to represent correlation between climate forcing and SLA variations. As a result, the NAO index is also examined. Positive NAO values are related to more immediate depressions in the Mediterranean Sea level, while negative ones to increased sea levels.

Noticing are the large positive NAO values at the beginning of 2002, 2007, 2008, 2011 2012 which are immediately depicted as depressions in the Mediterranean SLA with a time lag of less one-two months. The same behaviour is found for most winter months, i.e., a good correlation, while for summer months the response of the Mediterranean sea level to variations in NAO is not so well depicted (2002, 2004, 2006-2010 and 2012) [14], [15], [25], [27], [28], [29]. The response of sea to NAO variations indicates that NAO is more appropriate than SOI to describe the correlations between climate forcing and SLA variations.

4. REGRESSION ANALYSIS

A regional multiple regression analysis between Jason-1, Jason-2, and Cryosat-2 SLA variances with SOI, MOI and NAO indexes is carried out to model the response of the Mediterranean to these global and regional climatic phenomena. The b_1 coefficient corresponds to MOI, b_2 to SOI and b_3 to NAO so that a multiple regression model is outlined as in (Eq. 4).

$$C_0 = b_1 \times MOI + b_2 \times SOI + b_3 \times NAO \quad (4)$$

The values of the indexes have been normalized, using the minmax values of NAO, in order to construct values to be coherent to each other. All indexes values have been normalised to [0,1] through Eq. 5.

$$x' = \frac{X - X_{min}}{X_{max} - X_{min}}, \quad (5)$$

and then rescaled to [-1,1] through Eq. 6

$$x' = x' * 2 - 1 \quad (6)$$

Monthly values for Co and the normalised monthly value of each index are used in order to determine the three regression coefficients. In the tables below the values of each coefficient are presented.

Table 1: Regression coefficients for Cryosat-2

Year	b_1	b_2	b_3
2011	6.198	-3.055	1.128
2012	6.839	0.365	0.285
2013	8.564	1.182	1.586
2014	11.102	-1.335	-1.708

The correlation between SLA and the indexes depicted in Fig. 2 and Fig. 3 is similar to the values of the regression coefficients (Tab. 1 and Tab. 2). During all years, the coefficient of MOI takes the largest values, resulting in good correlation with the SLA. Especially, the SOI coefficient values are smaller, while during the years that the ENSO events are strong (2008, 2013) b_2 is larger than b_1 for the coefficients of Jason satellites. Finally, NAO coefficient b_3 generally takes small values signalling that the atmospheric and climate conditions in the North Atlantic are not the dominant contributing factor for the Mediterranean Sea. The large value for b_3 coefficient in 2010 for Jason satellite can be attributed to the small value of b_2 for the same year.

Table 2: Regression coefficients for Jason satellites

Sattelite	Year	b_1	b_2	b_3
JASON1	**2002**	6.198	-3.055	1.128
	2003	6.839	0.365	0.285
	2004	8.564	1.182	1.586
	2005	11.102	-1.335	-1.708
	2006	9.144	2.031	0.298
	2007	5.808	1.844	0.952
	2008	2.882	2.508	-1.371
JASON2	**2009**	5.234	3.032	0.209
	2010	6.143	0.666	3.407
	2011	2.464	3.362	-0.692
	2012	5.436	2.224	-0.958
	2013	-5.598	7.767	2.347
	2014	6.741	1.622	0.918

5. CORRELATION ANALYSIS

A correlation analysis is also carried out to model any seasonal correlation between SLA and these indexes. Four three-year periods (2002-2004, 2005-2007, 2008-2010, and 2011-2013) have been studied. Additionally, a monthly correlation for these periods was derived as well given the correlation coefficient $\rho_{X,Y}$ determined as:

$$\rho_{X,Y} = \frac{cov(X,Y)}{\sigma_X \sigma_Y}, \quad (7)$$

where cov is the covariance and σ_X is the standard deviation of X. The covariance cov is equal to

$$cov(X,Y) = E[(X - \mu_X)(Y - \mu_Y)], \quad (8)$$

where μ_X is the mean of X and E is the expectation. then Eq. 7 is derived as

$$\rho_{X,Y} = \frac{E[(X-\mu_X)-(Y-\mu_Y)]}{\sigma_X \sigma_Y}. \quad (9)$$

In this study X is the average variance of each three-year season of the period under study, μ_X the average of all seasons and σ_X the standard deviation while Y is the normalized index value for the same period.

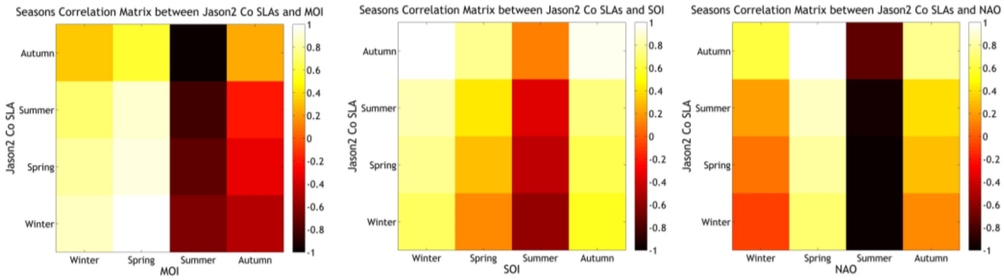

Figure 4: Seasonal correlation between Jason-2 SLA and MOI (left), SOI (middle) and NAO (right) for years 2011-2013.

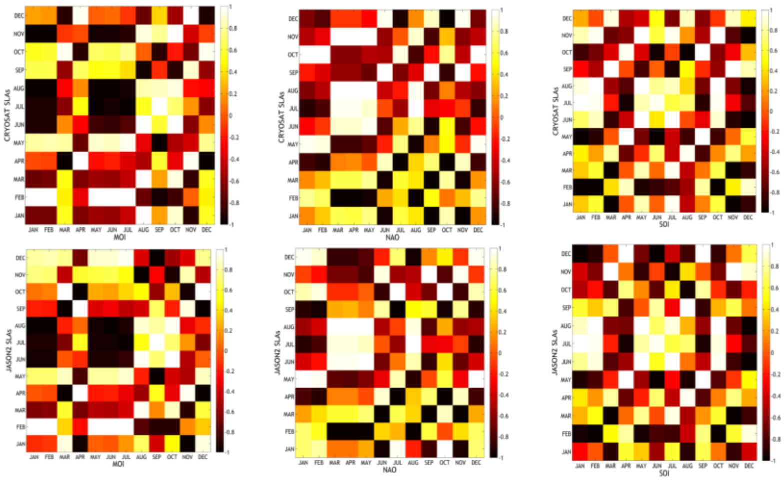

Figure 5: Monthly correlation between CRYOSAT and Jason-2 SLA and MOI (left), SOI (middle) and NAO (right) for year 2014.

In Fig. 4 correlation between seasons and indexes for a period of three years is depicted. Although a seasonal effect is not obvious, due to the fact that periods of three years are tested, it can be noticed that MOI and NAO are stronger correlated with SLA during the early months of each year (Winter-Spring). This is in line with the fact that NAO and MOI are well correlated and follow each other, especially during winter as has already depicted in Fig.2. On the other hand, the seasonal correlation between SOI and SLA depends on the strength of ENSO events and it is presented with a lag of 4-8 months. During the period under study in the figure above the ENSO events were weak and as a result, SLA and SOI are anti-correlated or they present weak correlation [7]. As already mentioned, a monthly correlation for these periods has been also examined between indexes and variances of both satellites. For monthly correlation in Eq. 9 *X*, *Y* are the monthly value of variance for each satellite and the normalised index monthly value.

In Fig.5 correlation between *Co* of both satellites (CryoSat-2 and Jason-2) and indexes for the same year is depicted (2014). Although a strong effect is not obvious, due to the fact that only one year is tested, it can be noticed that MOI is stronger correlated with SLA during the Spring-Summer months. Additionally, smaller correlation can be found and in early months of the year with NAO index. This is in line with the fact that NAO and MOI are well correlated and follow each other. On the other hand, the correlation between SOI and SLA depends on the strength of ENSO events and it is presented with a lag of 4-8 months. Finally, a very good agreement between correlations of both satellites is depicted for the same months in all cases.

6. PRINCIPAL COMPONENT ANALYSIS

In the last step of this study a Principal Component Analysis (PCA) between the variances of both satellites and oscillation indexes is performed. PCA or Empirical Orthogonal Function (EOF) is a method for analyzing the variability of a field. The method estimates EOF loading patterns and their variation on time, the PCs [8], [9], [10]. Data are organized in a matrix D $(n \times p)$ where n is the number of observations and p is the number of variables. In this study, D contains the monthly variances of each satellite for all years. The data matrix is decomposed by singular value decomposition through

$$\mathbf{D} = \mathbf{USV^T}, \tag{10}$$

where U and V are $(n \times n)$ and $(p \times p)$ matrices that satisfy $U^T U = I$ and $V^T V = I$, and S is a matrix of rank $r \leq min(n,p)$ whose diagonal contains the singular values $\sqrt{\lambda_i}$, $i=1,\dots,r$. The PC time series are obtained from the column vectors of the matrix P as

$$\mathbf{P} = \mathbf{US}. \tag{11}$$

PCA is usually performed to time-center data and this is achieved by removing the mean value from each column of $\boldsymbol{D}$. As a result the diagonal elements of matrix $\boldsymbol{S}$ are the variances explained by each PC. The PCs are ordered in terms of the percentage of the total variance explained. In the figures below the principal components of each satellite are depicted [20].

Fig. 6 presents the principal components for both satellites ordered in percentage of total data variance. For CryoSat-2 satellite the first and second principal component that contain ~70 and ~22% of the data variance are clearly distinguishable from the rest PCs. The third and fourth component contain less than 10 % of the data while the rest components are close to 0%. In the case of Jason satellites the first two components contain almost the 70% of the total variance while the third PC is almost 10%. The fourth and fifth component are close to 5% while the rest components are smaller. In order to investigate the low frequency signal and examine any possible contribution of global and regional climatic phenomena the PCs time series of each satellite and normalised indexes have been plotted [13].

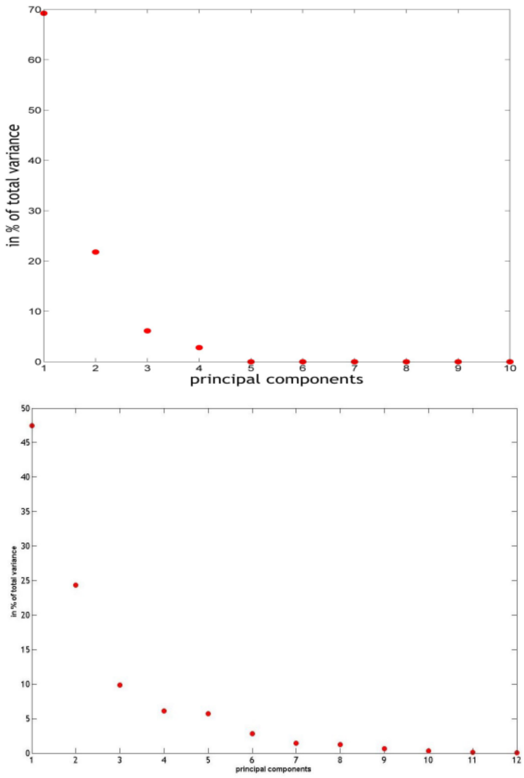

Figure 6: Jason (bottom) and CryoSat-2 (top) principal components.

In Fig.7 the first four PCs of *CryoSat-2* satellite and the first six PCs of Jason satellites are depicted. In both cases some correlation between MOI and PCs of satellites can be seen. For *CryoSat-2* satellite fourth PC is related to the MOI values while for Jason satellite the third PC follows the scaled MOI series. These two PCs are almost ~10% of the total variance as it can be seen in Fig. 6 representing seasonal and climatic signal modes. This correlation and agreement between MOI and SLA variances PCs signal that MOI is the dominant contributing factor for the Mediterranean Sea.

7. CONCLUSIONS

An analytical outline of the use of satellite altimetry data from the exact repeat missions of Jason-1, Jason-2 and CryoSat-2 satellites, in order to model the correlation between global and regional climatic phenomena, has been presented. The data analysed referred to records for a period of thirteen consecutive years (2002-2014, Jason satellites and 2010-2014, CryoSat-2) for the entire Mediterranean basin. A regional multiple regression, a correlation analysis and a Principal Component analysis between sea level anomalies and the SOI, MOI and NAO indexes was carried out to model any possible correlation between the Mediterranean sea level and these global and regional climatic phenomena. From the analysis of the empirical covariance functions of SLA, it was noticed that there is a significant annual variation, which is evident for the entire period under study with high values in January, lower values in spring due to reduced rainfall increasing values as summer progress due to snow melt and the thermal expansion in July-August. Finally the variance values decrease again in fall and start increasing in November due to higher level of precipitation.

Through regional multiple regression analysis between sea level anomalies and the SOI, MOI and NAO, it is obvious that the response of the Mediterranean Sea is more predominant with MOI. During years with strong ENSO events the regression coefficient for SOI index takes the biggest values. From the correlation analysis carried out, it was found that although a strong effect is not obvious, due to the fact that only one year is tested, it can be noticed that MOI is stronger correlated with SLA during the Spring-Summer months of each year. Additionally, smaller correlation can be found and in early months of the year with NAO index. This is in line with the fact that NAO and MOI are well correlated and follow each other. On the other hand, the correlation between SOI and SLA depends on the strength of ENSO events and it is presented with a lag of 4-8 months. Finally from the PCA analysis it was noticed that SLA PCs represent seasonal and climatic signal modes. Comparing the PCs with the indexes time series it can be concluded that Jason fourth and CryoSat-2 third principal component is related to the MOI index. Finally, the weak response of the SLA in the Mediterranean Sea level during summer signals that atmospheric forcing is not the contributing factor to the steric sea level variations in the Mediterranean during that period.

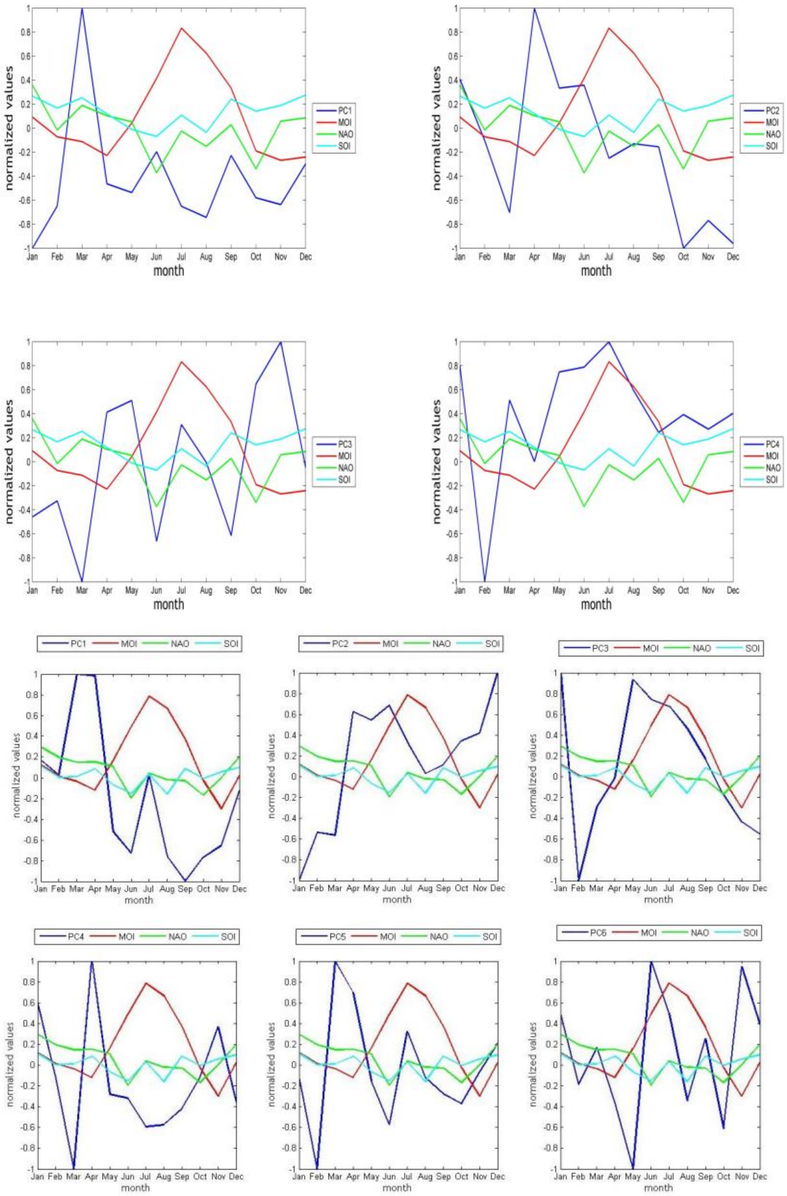

Figure 7: Principal components time series and scaled indexes for CryoSat-2 (top) and Jason (bottom).

8. REFERENCES

1. Allan, R.J., Nicholls, N., Jones, P.D. and Butterworth, I.J., (1991): A further extension of the Tahiti-Darwin SOI, early SOI results and Darwin pressure. *J. Climate* **4**, 743-749.
2. AVISO (2015) *OSTM/Jason-2 Products handbook* SALP-MU-M-OP-15815-CN, edition 1.9, May. 2015
3. AVISO User Handbook (2016) *Jason-1 Products Handbook* SMM-MU-M5-OP-13184-CN, edition 5.1, April 2016
4. Bureau of Meteorology, Australian Government (http://www.bom.gov.au).
5. Climatic Research Unit, University of East Anglia (http://www.cru.uea.ac.uk/)
6. Corte-Real J, Qian B, Xu H. (1998). Regional climate change in Portugal: precipitation variability associated with large-scale atmospheric circulation. *International Journal of Climatology* **18**: 619–635.
7. Golden Gate Weather Services (http://ggweather.com/)
8. Hotelling, H. (1933). Analysis of a complex of statistical variables into principal components. *Journal of Educational Psychology*, **24**, 417–441, and 498–520.
9. Hotelling, H. (1936). Relations between two sets of variates. *Biometrika*, 27, 321–77
10. Jolliffe (2002) I.T. Principal Component Analysis, Series: *Springer Series in Statistics*, 2nd ed., Springer, NY, 2002, XXIX, 487 p. 28 illus. ISBN 978-0-387-95442-4.

11. Knudsen P. (1988). Estimation and modelling of the local empirical covariance function using gravity and satellite data. *Bul. Geod*. 61:45-160.
12. Können, G.P., Jones, P.D., Kaltofen, M.H., and Allan, R.J., (1998): Pre-1866 extensions of the Southern Oscillation Index using early Indonesian and Tahitian meteorological readings. *J. Climate* **11**, 2325-2339.
13. O. De Viron, I. Panet, M. Diament (2006). Extracting low frequency climate signal from GRACE data. *eEarth*, 1 (1), pp.9-14.
14. Osborn, T.J., (2006) Recent variations in the winter North Atlantic Oscillation. *Weather* **61**, 353-355.
15. Osborn, T.J., (2011) Winter 2009/2010 temperatures and a record-breaking North Atlantic Oscillation index. *Weather* **66**, 19-21.
16. Palutikof, J.P., (2003). Analysis of Mediterranean climate data: measured and modelled. In: *Bolle, H.J.* (ed): Mediterranean climate: Variability and trends. Springer-Verlag, Berlin.
17. Pavlis N., Holmes S., Kenyon S., Factor J., (2012). The Development and Evaluation of the Earth Gravitational Model 2008 (EGM2008). *Journal of Geophysical Research*, Volume 117.
18. Perry, A.H. (2000). The North Atlantic Oscillation: an enigmatic see-saw. *Progress in Physical Geography* **24**, 289–94
19. RADS-DEOS (2015) Available from: http://rads.tudelft.nl (Radar Altimeter Database System). Accessed January 2015.
20. Rangelova, E., W. van der Wal, A. Braun, M. G. Sideris, and P. Wu (2007). Analysis of Gravity Recovery and Climate Experiment time-variable mass redistribution signals over North America by means of principal component analysis, *J. Geophys*. Res.,**112**, F03002, doi:10.1029/2006JF000615.
21. Ropelewski, C.F. and Jones, P.D., (1987). An extension of the Tahiti-Darwin Southern Oscillation Index. *Monthly Weather Review* **115**, 2161-2165.
22. Supic, M., B. Grbec, I. Vilibic, I. Ivancic (2004). Long-term changes in hydrodynamical conditions in Northern Adriatic and its relationship to hydrological and atmospheric processes. *Ann. Geophys*., **22** (3), pp. 733–745
23. Sušelj, K., K. Bergant (2006) Mediterranean Oscillation Index. *Geophys. Res*. Abstr., 8, p. 02145 European Geosciences Union.
24. Tscherning, C.C. & Rapp, R.H. (1974). Closed covariance expressions for gravity anomalies, geoid undulations, and deflections of the vertical implied by anomaly degree-variance models. *Reports of the Department of Geodetic Science*, **208**, The Ohio State University, Columbus, Ohio.
25. Tsimplis, M.N. and S.A. Josey (2001). Forcing of the Mediterranean Sea by atmospheric oscillations over the North Atlantic *Geophysical Research Letters* **28** (5): 803-806.
26. Tsimplis, M.N., Shaw A.G.P., (2008). The forcing of mean sea level variability around Europe, *Global and Planetary Change*, Volume **63**, Issues 2–3, September 2008, Pages 196-202, ISSN 0921-8181, 10.1016/j.gloplacha.2007.08.018.
27. Wakelin, S. L., P. L. Woodworth, R. A. Flather, J.A. Williams. (2003). Sea-level dependence on the NAO over the NW European Continental Shelf. *Geophysical Research Letters*, **30(7)**, Art. No. 1403.
28. Woolf, D.K., A.G.P. Shaw and M.N, Tsimplis (2003). The influence of the North Atlantic Oscillation on Sea Level Variability in the North Atlantic Region. *The Global Atmosphere and Ocean System*. **9(4):** 145-167.
29. Vergos, G.S., Natsiopoulos, D.A., (2012). Ocean remote sensing altimetric satellites in support of sea level anomalies and mean sea surface modeling. Presented at the 32nd European Association of Remote Sensing Laboratories (EARSel) Symposium “Advances in Geosciences”, May 21-24, Myconos, Greece.